

2011

# Multi-Cause Degradation Path Model: A Case Study on Rubidium Lamp Degradation

Sun Quan

Paul H. Kvam
*University of Richmond*, pkvam@richmond.edu



## Recommended Citation

Quan, Sun, and Paul H. Kvam. "Multi-cause Degradation Path Model: A Case Study on Rubidium Lamp Degradation." *Quality and Reliability Engineering International* 27, no. 3 (2011): 781-93. doi:10.1002/qre.1159.

Research Article

Quality and Reliability Engineering International

(wileyonlinelibrary.com) DOI: 10.1002/qre.1159

Published online 19 November 2010 in Wiley Online Library

# Multi-Cause Degradation Path Model: A Case Study on Rubidium Lamp Degradation

**Sun Quan[a]*† and Paul H. Kvam[b]**

**At the core of satellite rubidium standard clocks is the rubidium lamp, which is a critical piece of equipment in a satellite navigation system. There are many challenges in understanding and improving the reliability of the rubidium lamp, including the extensive lifetime requirement and the dearth of samples available for destructive life tests. Experimenters rely on degradation experiments to assess the lifetime distribution of highly reliable products that seem unlikely to fail under the normal stress conditions, because degradation data can provide extra information about product reliability. Based on recent research on the rubidium lamp, this article presents a multi-cause degradation path model, including its application background, model description, modeling method, and parameter estimation method. Using the available data from degradation tests, we construct point estimates and interval estimates for rubidium lamp lifetimes using regression techniques. Copyright © 2010 John Wiley & Sons, Ltd.**

**Keywords:** multi-cause degradation path model; rubidium lamp; reliability

## 1. Introduction

A state-of-the-art global navigation satellite system, such as GPS, GALILEO, GLONASS, can provide highly accurate, guaranteed global positioning services for industries, governments, and individuals around the world. Atomic clocks represent critical components of the satellite navigation system. An atomic clock is a sophisticated timekeeping device that uses an atomic resonance frequency standard as its timekeeping element. They are the most accurate time and frequency standards known, and are used as primary standards for international time distribution services, to control the frequency of television broadcasts, and in global navigation satellite systems such as GPS. The Rubidium Atomic Frequency Standard (RAFS) is at present the baseline clock technology for the global navigation satellite payload. According to this baseline, every satellite will embark at least two RAFSs. The adoption of a 'dual technology' for the on-board clocks is dictated by the need to ensure a sufficient degree of reliability (technology diversity) and to comply with the Galileo lifetime requirement (12 years) listed in Jeanmaire *et al.*[1] and Rochat *et al.*[2].

### 1.1. Background

The rubidium lamp is the core of the RAFS and other optically pumped devices. The conventional lamp used in the RAFS consists of a glass envelope containing a charge of the appropriate metal such as rubidium, and a buffer gas under a pressure of a few torr. The lamp is usually ignited by a radio frequency (RF) coil that surrounds the glass envelope. The spectral mission properties of the lamp have long been recognized as extremely important in the operation of optically pumped devices, and have been thoroughly studied by Cook and Frueholz[3]. When the rubidium atoms change energy levels for the RF discharge power, electrons in atoms will emit the precise microwave signal as the source of standard frequencies Figure 1 shows a typical rubidium discharge lamp. The lamp consists of a glass envelope that contains the excess rubidium metal and a buffer gas. An RF coil (not shown) surrounds the exposed portion of the glass envelop and sustains a plasma in the lamp.

Only a limited amount of rubidium can be placed in the lamp due to concerns over the stability of its output intensity. If the amount of rubidium contained in the lamp is depleted past a given threshold, the rubidium lamp will fail to operate. Several possible lamp failure mechanisms were investigated by Volk *et al.*[4] in response to the failures of the rubidium atomic clocks on board GPS satellites. These mechanisms included the quenching of the excited rubidium atoms, rubidium reaction with impurities, and the interaction of rubidium with the glass. Investigations reveal that the interaction of rubidium with the glass and the

[a]*Department of System Engineering, College of Information System and Management, National University of Defense Technology, Changsha, HN 410073, People's Republic of China*

[b]*H. Milton Stewart School of Industrial and System Engineering, Georgia Institute of Technology, Atlanta, GA 30318, U.S.A.*

**Correspondence to: Sun Quan, Department of System Engineering, College of Information System and Management, National University of Defense Technology, Changsha, HN 410073, People's Republic of China.*

†*E-mail: sunquan@nudt.edu.cn*

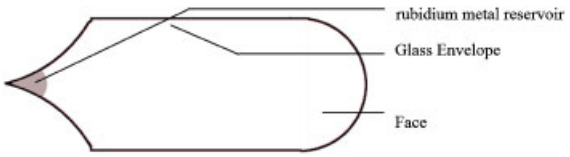


**Figure 1**. Typical rubidium discharge lamp

rubidium reaction with impurities are the two main reasons for rubidium depletion, and the interaction between the rubidium and the glass had depleted most of the rubidium[5].

### *1.2. The interaction of rubidium with the glass*

Cook and Frueholz[3] model the interaction of rubidium with the glass using the formula

$$Z(t)=2\cdot A\cdot C_0\cdot\left(\frac{\pi}{D}\right)\cdot\sqrt{t},\quad t>0, \tag{1}$$

where $A$ is the rubidium lamp surface area, $C_0$ is the density of the penetrating species at the glass surface, $D$ is the diffusion coefficient of the penetrating species for the particular glass, $Z(t)$ represents the total rubidium interaction amount to time $t$. The difficulty with Equation (1) exists in obtaining precise knowledge of both $C_0$ and $D$ in the lamp application. From Volk *et al.*[4], the density of rubidium at the glass surface certainly depends on the temperature of the rubidium reservoir that controls the rubidium vapor pressure in the lamp. However, based on a mathematical model of the discharge lamp, the density of rubidium at the lamp wall is also predicted to be a strong function of the RF drive power applied to the lamp.

Unfortunately, at present it is not possible to model the exact functional dependence of rubidium density on lamp drive power. Additionally, the diffusion coefficients for rubidium in glasses of interest are not well known. The analyses that we have performed on various lamps have not provided sufficiently detailed information with regard to the diffusion coefficients. The best way, to date, to determine the rate of rubidium diffusion into the glass envelope of a lamp is by performing rubidium depletion measurements under certain lamp conditions of interest as shown in Cook and Frueholz[3].

For convenience, we can write

$$Z(t)=b_0+a_0\cdot\sqrt{t},\quad t>0, \tag{2}$$

where $b_0$ represents the initial interaction amount, $a_0$ is equal to $2AC_0\pi/D$ in Equation (1).

### *1.3. Rubidium reaction with impurities*

Another postulated mechanism for the failure of the rubidium lamp was the loss of rubidium by reaction with species outgassed from the envelope to form non-volatile rubidium oxide ($Rb_2O$). The most likely reactions are:

$$2Rb+H_2O\rightarrow Rb_2O+H_2,$$

$$4Rb+O_2\rightarrow 2Rb_2O.$$

Through these reactions, 30 or more micrograms rubidium will be depleted. Although this amount of depletion is not significant in terms of the total charge of rubidium (300 μg or more), it should be taken into account to properly analyze the rubidium lamp's lifetime and its reliability.

A mathematical model of the rubidium reaction with impurities by Cook and Frueholz[3] is given as

$$W(t)=P\cdot(1-e^{-Q\cdot t}),\quad t>0, \tag{3}$$

where $P$ represents the total amount of rubidium lost through reaction, $Q$ is the reaction rate constant (as given in Volk *et al.*[4]), and $W(t)$ represents the total rubidium reaction amount to time $t$. From Equation (3), we know that $W(t)$ will tend to be infinitely close to a maximum amount ($P$) and the reaction with impurities can be considered as stopping when $t$ is long enough; hence, another mathematical model of the rubidium reaction with impurities can be given by

$$W(t)=b_1+a_1t,\quad t<T_1, \tag{4}$$

where $b_1$ represents the initial reaction amount and $a_1$ is the average reaction rate before the reaction stops by time $T_1$.

## 2. Rubidium degradation

The lifetime of a rubidium lamp is closely related to the amount of rubidium atoms in the lamp; see Frueholz[6] and Bhaskar[7]. A rubidium atom's interaction with the lamp envelope glass (diffusion into the lamp's glass wall) and its reaction with impurities

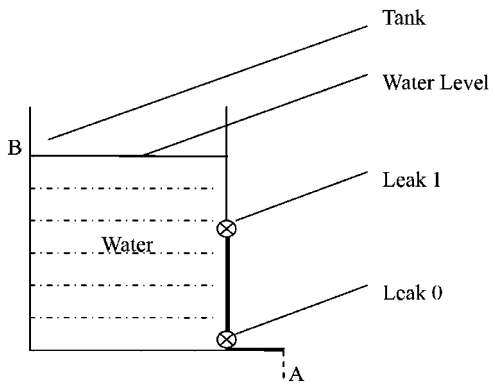


**Figure 2**. Water tank with leaks at bottom (Leak 0) and middle (Leak 1)

within the lamp will lead to the depletion of rubidium. When the amount of rubidium atom is depleted, the lamp's optical pumping will fail and the lamp fails.

Because of the challenges in obtaining lifetime data for rubidium lamps, the ability to analyze degradation measurements is paramount in accurately estimating lifetime distributions. The rubidium lamp is used only in some highly specialized equipment, such as satellites. Consequently, the demand for these lamps is low although it serves a critical purpose. In this case, the rubidium lamp is made in special laboratories, and due to manufacturing and economic constraints, there are few rubidium lamps that can be used in destructive life tests.

Recently, degradation data have been shown to be a superior alternative to lifetime data in most statistical analyses because they are potentially more informative. Freitas *et al.*[8] discuss two major aspects of modeling for degradation data. One approach is to assume that the degradation is a random process in time. Doksum[9] used a Wiener process model to analyze degradation data. Tang and Chang[10] modeled non-destructive accelerated degradation data from power supply units as a collection of stochastic processes. Whitmore and Shenkelberg[11] considered that the degradation process in the model is taken to be a Wiener diffusion process with a time-scale transformation. An alternative approach is to consider more general statistical models. Degradation in these models is modeled by a function of time and some possibly multidimensional random variables. These models are called 'general degradation path models'.

Lu and Meeker[12] developed statistical methods using degradation measures to estimate a time-to-failure distribution for a broad class of degradation models. They considered a nonlinear mixed-effects model (NMLE) and used a two-stage method to obtain point estimates and confidence intervals of percentiles of the failure-time distribution. Lu *et al.*[13] proposed a model with random regression coefficients and standard-deviation function for analyzing linear degradation data from semiconductors. Su *et al.*[14] considered a random coefficient degradation model with random sample size and used maximum likelihood (ML) for parameter estimation. Hamada[15] used a Bayesian approach for analyzing a laser degradation data. Bae and Kvam[16] proposed a change-point model for modeling incomplete burn-in during the production of display devices.

This aggregate of previous research has a focus on estimating the parameters in the degradation model along with the percentiles of the failure-time distribution, and these models all assume that degradation is due to either a single cause, or when there are multiple causes, they have an additive effect that can be modeled into a single additive model. In some cases, such assumptions are not suitable.

To illustrate a case in which the regular model assumptions do not hold, consider the water tank pictured in Figure 2. When there is no water, the tank will fail to operate. From Figure 2, we can see that there are two causes that lead to tank failure, labeled as Leak 0 (bottom) and Leak 1 (middle). These two different causes can be analyzed using a simple degradation model that assumes that a single cause exists, based on the water loss data observed from point A or tank water-level falling data which can be observed from point B. However, the causes for the two leaks are different. Leak 1 will stop when the water level is lower than a particular level, but Leak 0 will not stop until the water is completely gone.

Let $d_1(t)$ and $d_0(t)$ be the amount of leaking water leaking at time $t$ corresponding to Leak 1 and Leak 0. $Y(t)$, defined as the total water leaking amount at time $t$, can be described as

$$Y(t) = d_1(t) + d_0(t), \quad t > 0. \tag{5}$$

Suppose $d_1(t)$ and $d_0(t)$ are linear functions of $t$, so that the rate of water leaking from Leak 1 and Leak 0 is constant. Then,

$$d_1(t) = a_1 t + b_1, \quad 0 \le t \le T_1, \tag{6}$$

$$d_0(t) = a_0 t + b_0, \quad 0 \le t. \tag{7}$$

$T_1$ is the time at which Leak 1 ceases, when the water level is so low that there will be no water leaking from Leak 1. Then from Equations (5) to (7), we can get a crooked line as shown in Figure 3.

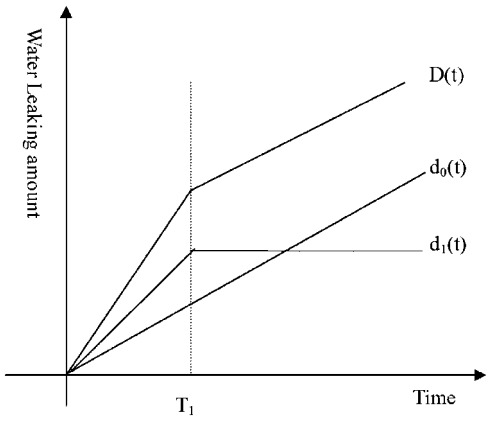


**Figure 3**. Amount of tank water leakage as a function of time

In fact, the degradation of the rubidium lamp can be compared with the loss of water in tank. In the lamp, there are also two disparate causes that lead to the depletion of rubidium. One cause is the reaction with impurities, but such a reaction will stop when the impurities are used up, which occurs long before the lamp fails. The other cause is the interaction with glass (diffusion), and this kind of diffusion will continue until all rubidium is completely depleted.

Bae and Kvam[16] proposed a model with a single change-point, and Sari *et al.*[17] proposed a two-stage model to analyze a similar problem in light displays. In the change-point model, several causes actually are integrated into one cause (path) and the degradation process is modeled as two independent phases between the change-point. In accelerated degradation tests, the degradation rate can be modified by changes in stress levels (such as temperature) and is probably different from cause to cause; hence, we would study these causes separately.

In this article, such a tank degradation problem or rubidium degradation problem will be called a *multi-cause degradation problem*, and we will develop a generalized multi-cause degradation path model to solve the multi-cause degradation problem.

## 3. Multi-cause degradation path model

For convenience, we will consider two kinds of causes in our generalized multi-cause degradation path model. One cause is limited degradation. When the limit is reached, the degradation is halted, like the way Leak 1 stops once the water in the tank goes below a fixed threshold. The other cause is unlimited degradation, meaning that the degradation process will persist until failure occurs. Leak 0 in the water tank is an example of unlimited degradation. Because of the continuity and similarity of independent sources of unlimited degradation, we can integrate all unlimited degradation processes into a single process. But for limited degradation processes, we cannot simply integrate them into one process if the thresholds are not identical.

Assume that there are $M+1$ causes of degradation, which we will call Cause 0, Cause 1, Cause 2,..., Cause M. Cause 0 is unlimited degradation with degradation process denoted by $d_0(t)$, $t>0$. Cause 1, Cause 2,..., Cause M represent limited degradation and we denote the limit threshold for the $i$th cause with $Df_i, i=1,...,M$, so that

$$d_i(t)=\begin{cases} f_i(t), & 0\le t\le T_i, \\ Df_i, & t>T_i, \end{cases} \tag{8}$$

where $T_i (i=1,...,M)$ is the time at which limitation is achieved. If $D(t)$ represents the item's degradation process, then

$$D(t)=\sum_{i=0}^{M} d_i(t). \tag{9}$$

According to the definition by Meeker and Escobar[18], we can express performance reliability as

$$R(t)=\Pr\{D(t)<D_f\}=\Pr\left\{\sum_{i=0}^{M} d_i(t)<D_f\right\}=\Pr\left\{d_0(t)<D_f-\sum_{i=1}^{M} f_i(t)\right\}\cdot\prod_{i=1}^{M}(1-F_i(t))$$

$$+\Pr\left\{d_0(t)<D_f-\sum_{i=1}^{M-1} f_i(t)-D_{f_M}\right\}\cdot\prod_{i=1}^{M-1}(1-F_i(t))\cdot F_M(t)$$

$$+\Pr\left\{d_0(t)<D_f-\sum_{i=1}^{M-2} f_i(t)-\sum_{i=1}^{2} D_{f_i}\right\}\cdot\prod_{i=1}^{M-2}(1-F_i(t))\cdot\prod_{i=1}^{2} F_{M-i+1}(t)$$

$$+\cdots+\Pr\left\{d_0(t)<D_f-\sum_{i=1}^{M-k}f_i(t)-\sum_{i=1}^{k}D_{f_i}\right\}\cdot\prod_{i=1}^{M-k}(1-F_i(t))\cdot\prod_{i=1}^{k}F_{N-i+1}(t)$$

$$+\cdots+\Pr\left\{d_0(t)<D_f-\sum_{i=1}^{M}D_{f_i}\right\}\cdot\prod_{i=1}^{M}F_{M-i+1}(t), \tag{10}$$

where $F_i(t)$ is the distribution function of $T_i$, $i=1,\ldots,M$.

## 4. Rubidium lamp life test

During the past years, in order to figure out the necessary requirements that will ensure reliable operation of the rubidium lamp, there have been a number of experiments undertaken by the China State Key Laboratory of Magnetic Resonance & Atomic & Molecular Physics. The lab collected various measurements to quantify the quality of the lamps, including degradation data which we feature in this article.

In one study, there were six lamps of the same type of glass put into degradation test. The first three lamps were tested for 28 800 h (3 years and 4 months). Figure 4 shows the measured amount of rubidium in lamps #1–#3. Note that the time measurement intervals are not identical. The next three lamps were tested with the same operating conditions as the first three, and testing began at the same date. Only after 1 year and 8 months of regular use, degradation measurements were made for the second group of lamps, which lasted for another 14 400 h (1 year and 8 months). Figure 5 shows the rubidium amount in lamps #4–#6, and again the time measurement intervals are not equal. Because these six lamps had worked under similar usage conditions, and all started work at the same time, we can combine the degradation test data as shown in Figure 6.

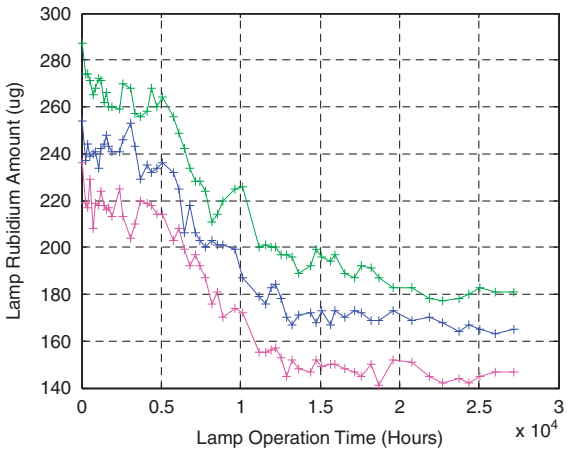


**Figure 4**. Rubidium amount of lamps #1–#3 (RF power = 2 W)

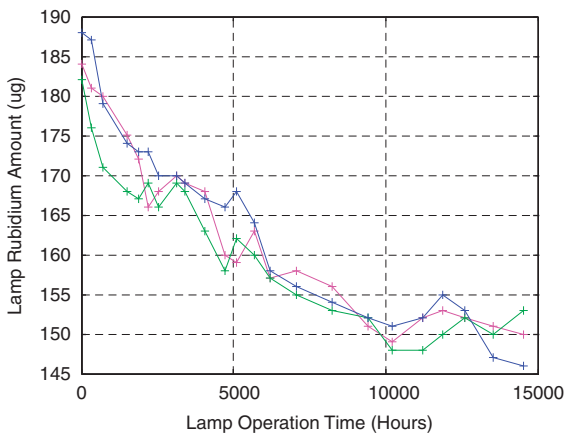


**Figure 5**. Rubidium amount of lamps #4–#6 (RF power = 2 W)

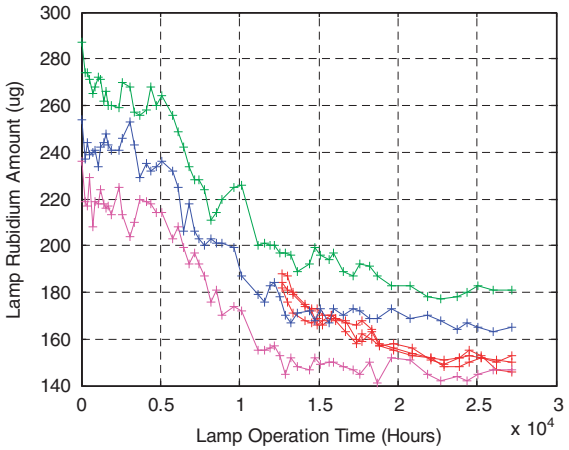


**Figure 6**. Rubidium amount of lamps #1–#6 (RF power = 2 W)

## 5. Multi-cause degradation path model of rubidium lamp

We know that the amount of rubidium in the rubidium lamp is affected by the initial amount of rubidium that exists in the lamp, as well as the reaction rate of the impurities and the glass interaction rate. First, in the satellite rubidium atomic clock, considering the rubidium lamp physical output's stability, there is a maximal initial fill amount that varies slightly for each lamp. Although the reaction between the rubidium and the impurities continues until the lamp stops working, this depletion occurs early in the lamp lifetime, and after a particular time, the rubidium amount depleted by the reaction of rubidium and impurities becomes negligible. In contrast, degradation due to the glass interaction will continue from the beginning to the end of lamp life.

### 5.1. *Parameter evaluating method*

For the rubidium lamp, there are two causes ($M+1=2$) leading to the degradation. One major cause is due to interaction with the glass, and its degradation path can be denoted as follows from Equation (2):

$$d_0(t)=Z(t)=b_0+a_0\cdot\sqrt{t},\quad t>0. \tag{11}$$

The other degradation cause is due to the reaction with impurities, and its degradation path can be denoted as follows from Equation (4):

$$d_1(t)=\begin{cases} W(t), & 0\le t\le T_1 \\ Df_1, & t>T_1 \end{cases} =\begin{cases} b_1+a_1\cdot t, & 0\le t\le T_1, \\ Df_1, & t>T_1. \end{cases} \tag{12}$$

From Equation (9), we obtain ($M=1$):

$$\begin{aligned} D(t)=\sum_{i=0}^{M} d_i(t)=d_0(t)+d_1(t)&=\begin{cases} b_0+a_0\cdot\sqrt{t}+b_1+a_1\cdot t, & 0\le t\le T_1, \\ b_0+a_0\cdot\sqrt{t}+Df_1, & t>T_1, \end{cases} \\ &=\begin{cases} (b_1+b_0)+a_0\cdot\sqrt{t}+a_1\cdot t, & 0\le t\le T_1, \\ (b_0+Df_1)+a_0\cdot\sqrt{t}, & t>T_1. \end{cases} \end{aligned} \tag{13}$$

For convenience, let

$$Y(t)=D_f-D(t),\quad c=D_f-b_1-b_0,\quad d=D_f-b_0-Df_1, \tag{14}$$

then Equation (13) can be written as

$$Y(t)=\begin{cases} c-a_1t-a_0\sqrt{t}, & 0\le t\le T_1, \\ d-a_0\sqrt{t}, & t>T_1, \end{cases} \tag{15}$$

where $Y(t)$ is a continuous function of time, $c$ represents the rubidium initial fill amount parameter, $a_1$ represents rubidium and impurities reaction parameter, $a_0$ represents the rubidium and glass interaction parameter, $T_1$ represents the intersection point at which limitation cause stops operating, and $c$, $a_1$, $a_0$, $d$, $T_1$ are all positive real numbers.

If $[t_{i-1}, t_i]$ represents the $i$th time interval, $i=1,\ldots,N$ (with $t_0=0$, $N$ is the test time intervals), and $Y(t_i)$ is the measured amount of rubidium in the lamp at time $t_i$, we can get the following equation from Equation (15):

$$Y(t_i)=\begin{cases} c-a_1 t_i-a_0\sqrt{t_i}+\varepsilon_1, & i=1,2,\ldots,\tau, \\ d-a_0\sqrt{t_i}+\varepsilon_2, t>T_1, & i=\tau+1,\ldots N, \end{cases} \tag{16}$$

where $(\varepsilon_1, \varepsilon_2)$ are the random measurement errors, assumed to be independent and identically distributed (iid) normal random variables with mean zero and variance $\sigma^2$. The parameter $\tau$ is the index corresponding to the intersection point $T_1$, with $\tau=1,\ldots,N$, and $t_\tau \le T_1 \le t_{\tau+1}$.

Additionally, under the continuity assumption for the degradation path, we can get

$$T_1=(c-d)/a_1, \tag{17}$$

where $d\varepsilon[c-a_1 t_{\tau+1}, c+a_1 t_{\tau+1}]$, $c\ge 0$, $a_1\ge 0$, $a_0\ge 0$, $d\ge 0$. Using the model described in Equation (17), it is possible to derive maximum likelihood estimators (MLEs) for $c$, $a_1$, $a_0$, $d$. The log-likelihood is given by:

$$L(c,a_1,a_0,d,\sigma^2,\tau)=\ln\frac{1}{(\sqrt{2\pi})^N\sigma^N}-\sum_{i=1}^{\tau}\frac{(y(t_i)-(c-a_1 t_i-a_0\sqrt{t_i}))^2}{\sigma^2}-\sum_{i=\tau+1}^{N}\frac{(y(t_i)-(d-a_0\sqrt{t_i}))^2}{\sigma^2}. \tag{18}$$

The procedure to obtain MLEs for the parameters in Equation (18) along with the corresponding estimate of $\tau$ can be summarized in a simple constrained optimization:

Find $\hat{c}$, $\hat{a}_1$, $\hat{a}_0$, $\hat{d}$, $\hat{\sigma}^2$, and $\hat{\tau}$ such that

$$L(\hat{c},\hat{a}_1,\hat{a}_0,\hat{d},\hat{\sigma}^2,\hat{\tau})=\sup L(c,a_1,a_0,d,\sigma^2,\tau), \tag{19}$$

subject to

$$\hat{T}_1=\frac{\hat{c}-\hat{d}}{\hat{a}_1} \quad \text{and} \quad \hat{d}\in[\hat{c}-\hat{a}_1 t_{\tau+1}, \hat{c}-\hat{a}_1 t_\tau],\ \hat{a}_1\ge 0,\ \hat{a}_0\ge 0,\ \hat{d}\ge 0,\ \hat{c}\ge 0.$$

Under the constraints above, the MLEs $\hat{c}$, $\hat{a}_1$, $\hat{a}_0$, $\hat{d}$, $\hat{\sigma}^2$ can be found in closed form:

$$\begin{aligned}\hat{c}=&\left\{\frac{T\cdot Y_\tau\cdot(N-\tau)+T_{N-\tau}^{1/2}\cdot T_{N-\tau}^{1/2}\cdot Y_\tau+Y_{N-\tau}\cdot T_{N-\tau}^{1/2}\cdot T_\tau^{1/2}-T_\tau^{1/2}\cdot YT^{1/2}\cdot(N-\tau)}{T_\tau^{3/2}\cdot T_\tau^{1/2}\cdot(N-\tau)-T\cdot T_\tau\cdot(N-\tau)-T_\tau\cdot T_{N-\tau}^{1/2}\cdot T_{N-\tau}^{1/2}}\right. \\ &\left.-\frac{2\cdot T\cdot YT_\tau\cdot(N-\tau)+2\cdot T_{N-\tau}^{1/2}\cdot T_{N-\tau}^{1/2}\cdot YT_\tau+T_{N-\tau}^{1/2}\cdot T_\tau^{3/2}\cdot Y_{N-\tau}-T_\tau^{3/2}\cdot YT^{1/2}\cdot(N-\tau)}{T_\tau^{3/2}\cdot T_\tau^{3/2}\cdot(N-\tau)-T_\tau^2\cdot T\cdot(N-\tau)-T_\tau^2\cdot T_{N-\tau}^{1/2}\cdot T_{N-\tau}^{1/2}}\right\}\Bigg/ \\ &\left\{\frac{\tau\cdot T\cdot(N-\tau)+\tau\cdot T_{N-\tau}^{1/2}\cdot T_{N-\tau}^{1/2}-T_\tau^{1/2}\cdot T_\tau^{1/2}\cdot(N-\tau)}{T_\tau^{1/2}\cdot T_\tau^{3/2}\cdot(N-\tau)-T_\tau T\cdot(N-\tau)-T_\tau\cdot T_{N-\tau}^{1/2}\cdot T_{N-\tau}^{1/2}}-\frac{T_\tau\cdot T\cdot(N-\tau)+T_\tau\cdot T_{N-\tau}^{1/2}\cdot T_{N-\tau}^{1/2}-T_\tau^{3/2}\cdot T_\tau^{1/2}\cdot(N-\tau)}{T_\tau^{3/2}\cdot T_\tau^{3/2}\cdot(N-\tau)-T_\tau^2\cdot T\cdot(N-\tau)-T_\tau^2\cdot T_{N-\tau}^{1/2}\cdot T_{N-\tau}^{1/2}}\right\},\end{aligned} \tag{20}$$

$$\hat{a}_1=\frac{2YT_\tau\cdot T.(N-\tau)+2YT_\tau\cdot T_{N-\tau}^{1/2}\cdot T_{N-\tau}^{1/2}+T_\tau^{3/2}\cdot Y_{N-\tau}\cdot T_{N-\tau}^{1/2}-T_\tau^{3/2}\cdot YT^{1/2}\cdot(N-\tau)}{T_\tau^{3/2}\cdot T_\tau^{3/2}\cdot(N-\tau)-T_\tau^2\cdot T\cdot(N-\tau)-T_\tau^2\cdot T_{N-\tau}^{1/2}\cdot T_{N-\tau}^{1/2}}-\frac{T_\tau\cdot T.(N-\tau)+T_\tau\cdot T_{N-\tau}^{1/2}\cdot T_{N-\tau}^{1/2}-T_\tau^{3/2}\cdot T_\tau^{1/2}\cdot(N-\tau)}{T_\tau^{3/2}\cdot T_\tau^{3/2}\cdot(N-\tau)-T_\tau^2\cdot T\cdot(N-\tau)-T_\tau^2\cdot T_{N-\tau}^{1/2}\cdot T_{N-\tau}^{1/2}}\cdot H,$$

$$\hat{a}_0=\frac{Y_{N-\tau}\cdot T_{N-\tau}^{1/2}-YT^{1/2}\cdot(N-\tau)+T_\tau^{1/2}\cdot(N-\tau)\cdot H-T_\tau^{3/2}\cdot(N-\tau)\cdot\hat{a}_1}{T\cdot(N-\tau)+T_{N-\tau}^{1/2}\cdot T_{N-\tau}^{1/2}},$$

$$\hat{d}=\frac{Y_{N-\tau}-T_{N-\tau}^{1/2}\cdot\hat{a}_0}{(N-\tau)},$$

$$\hat{\sigma}^2=\frac{2}{N}\left(\sum_{i=1}^{\tau}(y(t_i)-(c-\hat{a}_1\cdot t_i-\hat{a}_0\cdot\sqrt{t_i}))^2+\sum_{i=\tau+1}^{N}(y(t_i)-(\hat{d}-\hat{a}_0\cdot\sqrt{t_i}))^2\right),$$

where

$$T=\sum_{i=1}^{N}t_i,\quad T_\tau=\sum_{i=1}^{\tau}t_i,\quad T_{N-\tau}=\sum_{i=\tau+1}^{N}t_i,$$

$$T^{1/2}=\sum_{i=1}^{N}t_i^{1/2},\quad T_\tau^{1/2}=\sum_{i=1}^{\tau}t_i^{1/2},\quad T_{N-\tau}^{1/2}=\sum_{i=\tau+1}^{N}t_i^{1/2},$$

$$T^{3/2}=\sum_{i=1}^{N} t_i^{3/2},\ \ T_\tau^{3/2}=\sum_{i=1}^{\tau} t_i^{3/2},\ \ T_{N-\tau}^{3/2}=\sum_{i=\tau+1}^{N} t_i^{3/2},$$

$$T^{2}=\sum_{i=1}^{N} t_i^{2},\ \ T_\tau^{2}=\sum_{i=1}^{\tau} t_i^{2},\ \ T_{N-\tau}^{2}=\sum_{i=\tau+1}^{N} t_i^{2},$$

$$Y=\sum_{i=1}^{N} y(t_i)^{1/2},\ \ Y_\tau=\sum_{i=1}^{\tau} y(t_i),\ \ Y_{N-\tau}=\sum_{i=\tau+1}^{N} y(t_i),$$

$$YT^{1/2}=\sum_{i=1}^{N} y(t_i)\cdot t_i^{1/2},\ \ YT_\tau=\sum_{i=1}^{\tau} y(t_i)\cdot t_i,$$

$$H=\frac{T\cdot Y_\tau\cdot(N-\tau)+T_{N-\tau}^{1/2}\cdot T_{N-\tau}^{1/2}\cdot Y_\tau-(N-\tau)\cdot T_\tau^{1/2}\cdot YT^{1/2}+Y_{N-\tau}\cdot T_{N-\tau}^{1/2}\cdot T_\tau^{1/2}}{T_\tau^{3/2}\cdot T_\tau^{1/2}\cdot(N-\tau)-(N-\tau)\cdot T_\tau\cdot T-T_{N-\tau}^{1/2}\cdot T_{N-\tau}^{1/2}\cdot T_\tau}$$

$$-\frac{2T\cdot YT_\tau\cdot(N-\tau)+2T_{N-\tau}^{1/2}\cdot T_{N-\tau}^{1/2}\cdot YT_\tau-(N-\tau)\cdot T_\tau^{3/2}\cdot YT^{1/2}+Y_{N-\tau}\cdot T_{N-\tau}^{1/2}\cdot T_\tau^{3/2}}{T_\tau^{3/2}\cdot T_\tau^{3/2}\cdot(N-\tau)-(N-\tau)\cdot T_\tau^{2}\cdot T-T_{N-\tau}^{1/2}\cdot T_{N-\tau}^{1/2}\cdot T_\tau^{2}}.$$

Using $\hat{c}$, $\hat{a}_1$, $\hat{a}_0$, $\hat{d}$, $\hat{\sigma}^2$, and $\hat{\tau}$ in Equation (20), from Equation (14), we can also get the estimators for $b_0$, $b_1$ as follows:

$$\begin{aligned}\hat{b}_0&=D_f-D_{f_1}-\hat{d},\\ \hat{b}_1&=\hat{d}+Df_1-\hat{c}.\end{aligned}\tag{21}$$

### 5.2. Parameter evaluation

With a sample of $L$ lamps, we can obtain MLEs, along with the corresponding estimates their standard errors, for each lamp, treating the parameters as fixed effects unique to each lamp. From Equations (20) and (21), we would have a set of 5L parameters, assuming that the $j$th lamp's degradation parameters are $a_{0,j}$, $b_{0,j}$, $a_{1,j}$, $b_{1,j}$, $T_{1,j}$, $j=1,2,\ldots,L$.

With the data from the lamp study, using the degradation data shown in Figures 4–6, we obtain the multi-cause degradation path model parameter estimates and the standard errors for each individual lamp (listed in Table I), where $L=6$ and $Df_1=60\,\mu g$. For details about how the standard errors of nonlinear parameters can be efficiently computed; see Bates and Watts[19], for example.

To see if the parameter estimates follow the normal distribution, we used two tests for goodness of fit on the sets of six estimated coefficients: Lilliefor's test and the Anderson–Darling test. Treated as a sample data of random coefficients $b_0$ ($b_{0,j}$, $j=1,2,\ldots,6$), both tests indicate an adequate fit to a normal distribution at the 5% level. The other coefficients ($a_{0,j}$, $j=1,2,\ldots,6$), ($a_{1,j}$, $j=1,2,\ldots,6$), ($b_{1,j}, j=1,2,\ldots,6$), ($T_{1,j}$, $j=1,2,\ldots,6$) also passed this Lilliefor's test for goodness of fit to a normal distribution at the 5% level.

Unlike these other coefficients, $T_1$ represents the end (lifetime) of Rubidium reaction with impurities in the multi-cause rubidium degradation path model. Based on the results of Lilliefor's test of an exponential distribution, ($T_{1,j}$, $j=1,2,\ldots,6$) is adequately fit

**Table I**. The MLEs and their standard errors for parameters in the rubidium lamps' degradation model

| | $b_{1,j}$ | $a_{1,j}$ | $b_{0,j}$ | $a_{0,j}$ | $T_{1,j}$ | $\sigma_j^2$ |
|---|---|---|---|---|---|---|
| $j=1$ | 0.44 | 0.00456 | 69.27 | 0.09779 | 15270.1 | 88.8 |
| SE | 3.867 | 0.001334 | 2.4384 | 0.01544 | | |
| $j=2$ | 7.09 | 0.00326 | 9.58 | 0.25628 | 16220.2 | 99.14 |
| SE | 2.5726 | 0.001401 | 6.279 | 0.012928 | | |
| $j=3$ | 5.94 | 0.00372 | 37.3 | 0.23513 | 14547.5 | 84.17 |
| SE | 3.8502 | 0.001063 | 1.3947 | 0.013793 | | |
| $j=4$ | 2.15 | 0.00363 | 18.49 | 0.44789 | 15956.9 | 12.47 |
| SE | 0.17275 | 0.000376 | 2.7654 | 0.005813 | | |
| $j=5$ | 22.95 | 0.00224 | 26.24 | 0.40319 | 16561.6 | 14.77 |
| SE | 0.14349 | 0.000766 | 2.8393 | 0.007648 | | |
| $j=6$ | 2.05 | 0.00374 | 0.06 | 0.57030 | 15475.6 | 11.11 |
| SE | 0.53403 | 0.002852 | 0.64325 | 0.028464 | | |

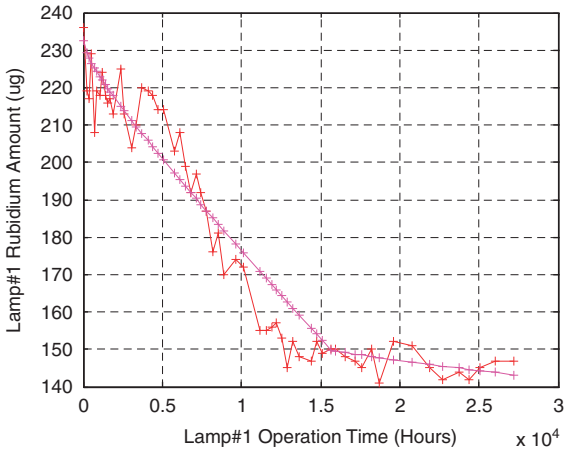


**Figure 7**. The degradation paths of rubidium lamps #1

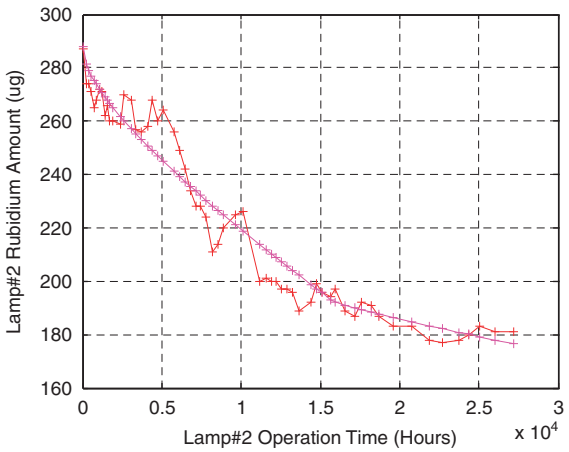


**Figure 8**. The degradation paths of rubidium lamps #2

by the exponential distribution at the 5% level. The resulting model now considers

$$a_0 \sim N(\mu_{a_0}, \sigma^2_{a_0}), \quad b_0 \sim N(\mu_{b_0}, \sigma^2_{b_0}), \quad a_1 \sim N(\mu_{a_1}, \sigma^2_{a_1}),$$
$$b_1 \sim N(\mu_{b_1}, \sigma^2_{b_1}), \quad T_1 \sim E(\lambda_1),$$

and we seek to calculate the estimates of $\mu_{a_0}$, $\sigma^2_{a_0}$, $\mu_{b_0}$, $\sigma^2_{b_0}$, $\mu_{a_1}$, $\sigma^2_{a_1}$, $\mu_{b_1}$, $\sigma^2_{b_1}$, $\lambda_1$.

By substituting the parameter estimates in Table I into Equation (13), the model generates the degradation path of each rubidium lamp, as shown from Figures 7 to 12.

## 6. Reliability analysis of rubidium lamp

In this section, we will use the degradation data to analyze the reliability of rubidium lamps. From Equation (10), when $M=1$, we can obtain the reliability performance of the rubidium lamp as follows:

$$\begin{aligned} R(t) &= \Pr\{D(t)<D_f\} \\ &= \Pr\{d_0(t)+d_1(t)<D_f\} \\ &= \Pr\{a_0\sqrt{t}+b_0+a_1\cdot t+b_1<D_f\}\cdot(1-F_1(t))+\Pr\{a_0\sqrt{t}+b_0<D_f-D_{f_1}\}\cdot F_1(t) \end{aligned} \tag{22}$$

From Equation (22), $D_f$ and $D_{f1}$ represent relative thresholds. For the rubidium lamp in this study, Cook and Frueholz[3] and Volk *et al.*[4] suggest that $D_f$ should be set to 300 μg and $D_{f1}$ should be set to 60 μg. Then the rubidium lamp's performance

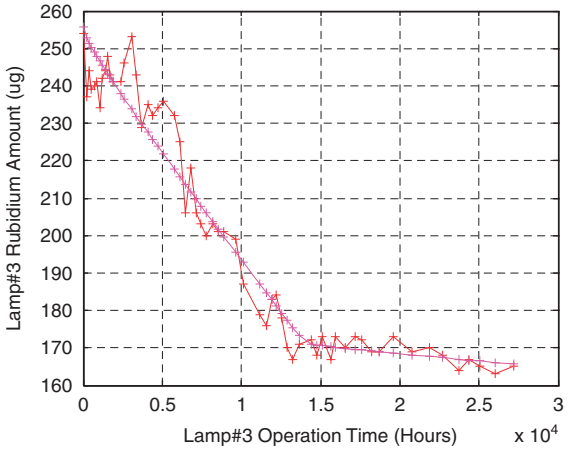


**Figure 9**. The degradation paths of rubidium lamps #3

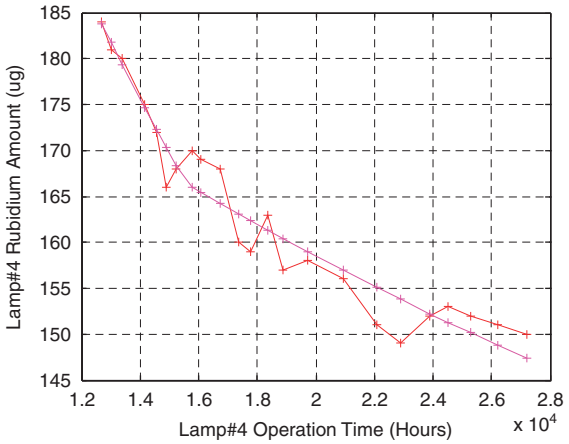


**Figure 10**. The degradation paths of rubidium lamps #4

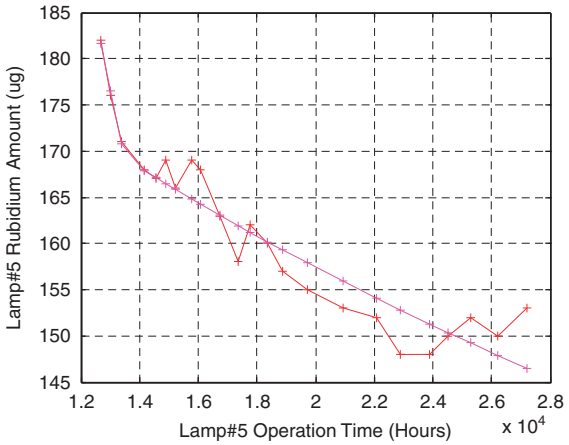


**Figure 11**. The degradation paths of rubidium lamps #5

reliability is calculated as:

$$R(t)=\Phi\left(\frac{D_f-(\mu_{a_0}\sqrt{t}+\mu_{a_1}t+\mu_{b_0}+\mu_{b_1})}{\sqrt{\sigma_{a_0}^2 t+\sigma_{a_1}t^2+\sigma_{b_0}^2+\sigma_{b_1}^2}}\right)e^{-\lambda_1 t}+\Phi\left(\frac{D_f-D_{f_1}-(\mu_{a_0}\sqrt{t}+\mu_{b_0})}{\sqrt{\sigma_{a_0}^2 t+\sigma_{b_0}^2}}\right)(1-e^{-\lambda_1 t}), \tag{23}$$

where $\Phi$ is the CDF of the Standard Normal Distribution.

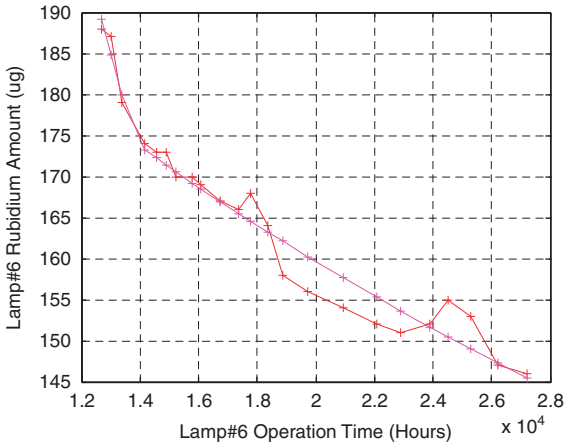


**Figure 12**. The degradation paths of rubidium lamps #6

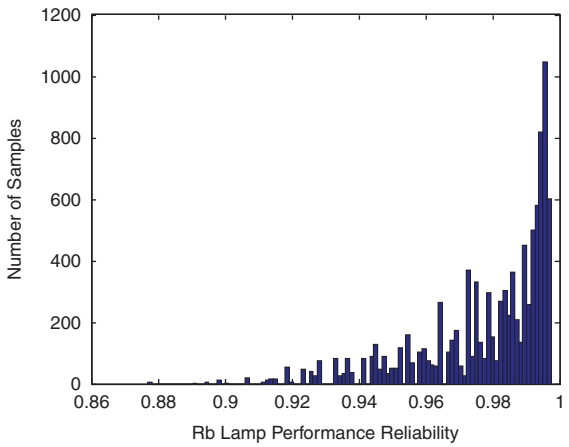


**Figure 13**. Rubidium lamp performance reliability's histogram by bootstrap data samples

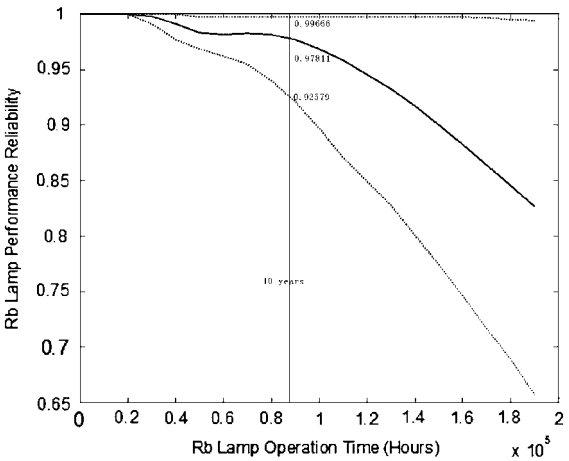


**Figure 14**. Estimated performance reliability of rubidium lamp along with 95% confidence interval

To get the performance reliability point estimation at time $t$, we first compute estimates of $\mu_{a_0}$, $\sigma^2_{a_0}$, $\mu_{b_0}$, $\sigma^2_{b_0}$, $\mu_{a_1}$, $\sigma^2_{a_1}$, $\mu_{b_1}$, $\sigma^2_{b_1}$, $\lambda_1$, and then substitute these estimates into Equation (23). When $D_f = 300\,\mu g$, $D_{f_1} = 60\,\mu g$, $t = 87\,600$ h (10 years), using a non-parametric bootstrap resampling method, we draw 10 000 bootstrap samples from the data set of Table I. Next, we compute statistical estimates for each sample using Equation (23), and return the results, which are illustrated in Figure 13. From the bootstrap samples, we use the 0.025 and 0.975 quantiles to form the confidence interval for the reliability estimate. For example, at 10 years (see Figure 14) we compute $R_{0.025} = 0.92579$ and $R_{0.975} = 0.99666$.

Applying this resampling technique at various operating times, $R(t)$ and its 95% bootstrap confidence intervals are plotted in Figure 14. The intervals are based on 10 000 bootstrap samples, the upper curve is $R(t)$ estimation for quantile = 0.025, the lower curve is $R(t)$ estimation for quantile = 0.975, and the middle curve is the reliability estimate.

## 7. Conclusions and future research

Owing to the previous lack of failure data, reliability estimation for the rubidium lamp has faced great hurdles. Using the data provided by the China State Key Laboratory, this article presents a multi-cause degradation path model, including its brief application background, model description, modeling method, and parameter estimation method. Using degradation data from just six life tests, we analyzed the performance reliability of the rubidium lamp and displayed the performance reliability results (point estimation and interval estimation).

As a result, this research represents that the first time rubidium lamp reliability has been inferred using degradation data. We note that the results are not completely reassuring. Previous internal lab studies based on theoretical models were comparatively optimistic about predicting lamp reliability. The reliability estimates here suggest that the rubidium lamp's performance reliability is lacking, with the lower confidence interval bound of 92% for 10 service years, which is over the tolerated failure frequency. As a matter of fact, from the rubidium lamp's multi-cause degradation path model and its performance reliability equation, we know that we need to make improvements in many aspects such as increasing the initial fill amount, decreasing the amount of impurities, and improving the glass materials, for example.

It is likely that multi-cause degradation is increasingly prevalent in degradation tests of highly complex devices, but mostly for convenience we integrated all causes into one cause and set up a degradation path that is easier to characterize. For the rubidium lamp, the high RF power will create different effects for the rubidium interaction with impurities as well as with glass, and the multi-cause degradation path model can help to recognize the difference between these effects. In future work, when more refined data become available, we will consider more specialized models of degradation that consider more causes of degradation.

## Acknowledgements

This work was supported by the National Science Foundation of China under agreement 60701006 and the National Science Foundation of the United States (CMMI-0700131).

## References

1. Jeanmaire A, Rochat P, Emma F. Rubidium atomic clock for Galileo. *Thirty-first Annual Precise Time and Time Interval* (*PTTI*) *Meeting*, Dana Point, CA, U.S.A., 1999; 627–636.
2. Rochat P, Droz F, Mosset P, Barmaverain G, Wang Q, Boving D. The onboard Galileo rubidium and passive maser, status and performance. *Proceedings of 2005 Joint IEEE International Frequency and Control Symposium and Precise Time and Time Interval* (*PTTI*) *Systems and Applications Meeting*, Vancouver, Canada, 2005; 26–32.
3. Cook RA, Frueholz RP. An improved rubidium consumption model for discharge lamps used in rubidium frequency standards. *Forty-second Annual Frequency Control Symposium*, Baltimore, MD, U.S.A., 1988; 525–531.
4. Volk CH, Frueholz RP, English TC, Lynch TJ, Riley WJ. Lifetime and reliability of rubidium discharge lamps for use in atomic frequency standard. *Thirty-eighth Annual Frequency Control Symposium*, Paris, France, 1984; 387–400.
5. IEEE Std. 1193–1994. IEEE Guide for measurement of environmental sensitivities of standard frequency generators [S]. *IEEE Std. 1193–1994*, 1994.
6. Frueholz RP. The effects of ambient temperature fluctuations on the long term frequency stability of a miniature rubidium atomic frequency standard. *IEEE International Frequency Control Symposium*, Boston, MA, U.S.A., 1996; 1017–1022.
7. Bhaskar ND. A historical review of atomic frequency standards used in space systems. *Proceedings of the 1996 IEEE International Frequency Control Symposium*, Boston, MA, U.S.A., 1996; 24–32.
8. Freitas MA, de Toledo ML, Colosimo EA, Pires MC. Using degradation data to assess reliability: A case study on train wheel degradation. *Quality and Reliability Engineering International* 2009; **25**:607–629.
9. Doksum KA. Degradation rate models for failure time and survival data. *CWI Quarterly* 1991 **4**:195–203.
10. Tang LC, Chang DS. Reliability prediction using nondestructive accelerated degradation data: Case study on power supplies. *IEEE Transactions on Reliability* 1995; **44**:562–566.
11. Whitmore GA, Shenkelberg F. Modeling accelerated degradation data using Wiener diffusion with a time scale transformation. *Lifetime Data Analysis* 1997; **3**:27–45.
12. Lu CJ, Meeker WQ. Using degradation measures to estimate a time-to-failure distribution. *Technometrics* 1993; **35**:161–174.
13. Lu JC, Park J, Yang Q. Statistical inference of a time-to-failure distribution from linear degradation data. *Technometrics* 1997; **39**:391–400.
14. Su C, Lu JC, Chen D, Hughes-Oliver JMA. Random coefficient degradation model with random sample size. *Lifetime Data Analysis* 1999; **5**:173–183.
15. Hamada M. Using degradation data to assess reliability. *Quality Engineering* 2005; **17**:615–620.
16. Bae SJ, Kvam PH. A change-point analysis approved to the modeling of incomplete burn-in during the production of display devices. *IIE Transactions* 2006; **6**:489–498.
17. Sari JK, Newby MJ, Brombacher AC, Tang LC. Bivariate constant stress degradation model: LED lighting system reliability estimation with two-stage modeling. *Quality and Reliability Engineering International* 2009; **8**:1067–1088.
18. Meeker WQ, Escobar LA. *Statistical Methods for Reliability Data*. Wiley: New York, 2003.
19. Bates DM, Watts DG. *Nonlinear Regression Analysis and its Applications*. Wiley: New York, 1988.

*Authors' biographies*

**Sun Quan** is Associate Professor in the College of Information System & Management at National University of Defense Technology (NUDT), China. From March 2009 to March 2010, he worked at Georgia Institute of Technology as a visiting scholar. He received his BS in Mathematics from NUDT at 1994, MS in Operation Research from NUDT at 1997, and PhD in System Engineering from NUDT at 2005. His research interests are in quality & reliability engineering. He is a member of IEEE.

**Paul H. Kvam** is Professor in School of Industrial and Systems Engineering at Georgia Institute of Technology. He received his BS in Mathematics from the Iowa State University in 1984, MS in Statistics from the University of Florida in 1986, and PhD in Statistics from the University of California, Davis in 1991. His research interests focus on statistical reliability with applications to engineering, nonparametric estimation, and analysis of complex and dependent systems. He has served as an associate editor for IEEE Transactions on Reliability (1992–2000), Technometrics (1999–2005), The American Statistician (2005–present) and Journal of the American Statistical Association (2002–present). He is a Fellow of the American Statistical Association, as well as an active member of Institute of Mathematical Statistics and Institute for Operations Research and Management Science.